

## Investigation of Strain-Promoted Azide-Alkyne Cycloadditions in Aqueous Solutions by Capillary Electrophoresis

Jana Steflova, Golo Storch, Sarah Wiesner, Skrollan Stockinger, Regina Berg, and Oliver Trapp

*J. Org. Chem.*, **Just Accepted Manuscript** • DOI: 10.1021/acs.joc.7b02092 • Publication Date (Web): 26 Dec 2017

Downloaded from <http://pubs.acs.org> on December 29, 2017

### Just Accepted

“Just Accepted” manuscripts have been peer-reviewed and accepted for publication. They are posted online prior to technical editing, formatting for publication and author proofing. The American Chemical Society provides “Just Accepted” as a free service to the research community to expedite the dissemination of scientific material as soon as possible after acceptance. “Just Accepted” manuscripts appear in full in PDF format accompanied by an HTML abstract. “Just Accepted” manuscripts have been fully peer reviewed, but should not be considered the official version of record. They are accessible to all readers and citable by the Digital Object Identifier (DOI®). “Just Accepted” is an optional service offered to authors. Therefore, the “Just Accepted” Web site may not include all articles that will be published in the journal. After a manuscript is technically edited and formatted, it will be removed from the “Just Accepted” Web site and published as an ASAP article. Note that technical editing may introduce minor changes to the manuscript text and/or graphics which could affect content, and all legal disclaimers and ethical guidelines that apply to the journal pertain. ACS cannot be held responsible for errors or consequences arising from the use of information contained in these “Just Accepted” manuscripts.

1  
2  
3  
4  
5  
6  
7  
8  
9  
10  
11  
12  
13  
14  
15  
16  
17  
18

# Investigation of Strain-Promoted Azide-Alkyne Cycloadditions in Aqueous Solutions by Capillary Electrophoresis

19  
20  
21  
22  
23  
24  
25  
26  
27  
28  
29

*Jana Steflova,<sup>\*,†,‡</sup> Golo Storch,<sup>†</sup> Sarah Wiesner,<sup>†</sup> Skrollan Stockinger,<sup>†</sup> Regina Berg<sup>†</sup> and Oliver Trapp<sup>\*,†</sup>*

<sup>†</sup>Department Chemie, Ludwig-Maximilians-Universität München,

Butenandtstr. 5–13, 81377 München, Germany

[oliver.trapp@cup.uni-muenchen.de](mailto:oliver.trapp@cup.uni-muenchen.de)

30  
31  
32  
33  
34  
35  
36  
37  
38  
39

<sup>‡</sup>Charles University, Faculty of Science, Department of Physical and Macromolecular Chemistry, Hlavova  
8, 128 40 Prague 2, Czech Republic

[svobod.j@natur.cuni.cz](mailto:svobod.j@natur.cuni.cz)

## Abstract

40  
41  
42  
43  
44  
45  
46  
47  
48  
49

The Cu-free 1,3-dipolar cycloaddition of cyclooctynes and azides is an up-and-coming method in bioorganic chemistry and other disciplines. However, broad application is still hampered by major drawbacks such as poor solubility of the reactants in aqueous media and low reaction rates.

50  
51  
52  
53  
54  
55  
56  
57

It is thus of high demand to devise a fast and user-friendly strategy for the optimization of reaction conditions and reagent design. We describe a capillary electrophoresis (CE) study of reaction kinetics in strain-promoted azide-alkyne cycloadditions (SPAAC) using substrates with

1  
2  
3 acidic or basic functionalities. This study reveals that the pH value has a significant effect on  
4  
5 reaction rates as a result of changes in the reactants' charge state via protonation or  
6  
7 deprotonation, and the concomitant changes of electronic properties.  
8  
9

10 This novel experimental setup also enables the study of even more challenging conditions like  
11  
12 reactions in micelles and we did indeed observe much faster SPAAC reactions in the presence of  
13  
14 surfactants. Careful combination of the above-mentioned parameters resulted in the identification  
15  
16 of conditions enabling remarkable rate enhancement by a factor of 80. This electrophoretic  
17  
18 method may thus serve as a versatile, fast and reliable tool for screening purposes in all research  
19  
20 areas applying SPAAC reactions.  
21  
22  
23  
24  
25  
26

## 27 **Introduction**

28  
29  
30 Click chemistry is a concept that describes high-yielding and extremely chemo-, regio- and  
31  
32 stereoselective chemical transformations that do neither require the exclusion of water and air nor  
33  
34 chromatographic purification procedures.<sup>1</sup> Despite this rather broad definition, the term Click  
35  
36 reaction is often used synonymously for the Cu(I)-catalyzed Huisgen azide-alkyne cycloaddition  
37  
38 (CuAAC).<sup>2,3</sup> 1,3-Dipolar cycloadditions of azides and alkynes resulting in the formation of 1,2,3-  
39  
40 triazoles had been developed by Huisgen in the 1960s.<sup>4-8</sup> However, in the absence of any catalyst  
41  
42 this reaction only proceeds under harsh conditions with low reaction rates giving a mixture of  
43  
44 1,4- and 1,5-disubstituted 1,2,3-triazole regioisomers. In 2002, the group of Meldal presented a  
45  
46 copper(I)-catalyzed solid-phase synthesis of 1,2,3-triazoles.<sup>9</sup> At the same time, the group of  
47  
48 Sharpless independently reported on a copper(I)-catalyzed azide-alkyne cycloaddition under  
49  
50 solution phase conditions, most interestingly also in aqueous media.<sup>2</sup> Based on the development  
51  
52 of more and more advanced ligand systems (NHC, iminophosphoranes, tris(triazolyl)methanol),  
53  
54  
55  
56  
57

1  
2  
3 there have also been several examples of CuAAC reactions being performed in water and under  
4 aerobic conditions.<sup>10-12</sup> Experimental and DFT-based mechanistic investigations have shown the  
5 copper(I)-catalyzed variant of the Huisgen cycloaddition to proceed by a stepwise mechanism  
6  
7  
8  
9  
10 with activation of the alkyne by coordination to two copper(I) ions.<sup>13-17</sup> Since 2002, the CuAAC  
11 reaction has rapidly found a plethora of applications in chemistry and related disciplines, among  
12 them many in biological sciences.<sup>18-24</sup> In particular, the CuAAC reaction is widely used for  
13  
14  
15 coupling a biomolecule to another (bio)molecule via a covalent molecular linker  
16  
17  
18 (bioconjugation), as its characteristics and reaction conditions are compatible with some of the  
19 requirements and conditions in this field (bioorthogonality),<sup>25-27</sup> *i.e.* tolerance towards air and  
20  
21  
22 aqueous media of physiological pH, ambient temperature, biological and chemical inertness of  
23  
24  
25 the starting materials and the cycloadduct, rapid and full conversion, and high specificity.  
26  
27  
28 However, the reaction's major limitation in biological contexts lies in the use of a transition metal  
29  
30  
31 catalyst, as Cu(I) ions have been shown to be toxic for isolated cells as well as for living  
32  
33  
34 organisms due to oxidative damage.<sup>28,29</sup> For this reason there is a strong interest in developing  
35  
36  
37 suitable alternatives for CuAAC compatible with this additional requirement of bioorganic  
38  
39  
40 applications (non-toxicity).

41  
42 In 2004, the group of Bertozzi developed a *Strain-Promoted [3+2] Azide-Alkyne Cycloaddition*  
43 (SPAAC) applying cyclooctyne dipolarophiles in order to increase the rate of reaction by taking  
44  
45  
46 advantage of the lower activation energy as a result of the strained substrate geometry in  
47  
48  
49 connection with an early – and thus substrate-like – transition state (according to the Hammond  
50  
51  
52 postulate).<sup>27,30,31</sup> This idea has its foundations in reports by Blomquist and Liu (1953) and by  
53  
54  
55 Wittig and Krebs (1961), both describing the explosion-like 1,3-cycloaddition of cyclooctyne  
56  
57  
58 with phenyl azide.<sup>32,33</sup> The high reactivity of cyclooctynes in comparison to acyclic or unstrained  
59  
60  
61 cyclic alkynes is explained by destabilization of the ground state due to substantial bond angle

1  
2  
3 distortion, which leads to a lower activation energy for the cycloaddition reaction.<sup>34-36</sup> The  
4 SPAAC has been accelerated by introduction of electron-withdrawing fluoride substituents  
5 (mono- and difluorinated cyclooctyne substrates, MOFOs and DIFOs).<sup>37-39</sup> Substantial rate  
6 enhancement in SPAAC reactions was also achieved by using dibenzocyclooctyne (DIBO or  
7 DBCO),<sup>40</sup> difluorobenzocyclooctyne (DIFBO),<sup>41</sup> azadibenzocyclooctyne (DIBAC)<sup>42</sup> or  
8 biarylazacyclooctynone (BARAC) substrates.<sup>43,44</sup>

9  
10  
11  
12  
13  
14  
15  
16  
17 However, there is still demand for improvement of the SPAAC, as even with state-of-the-art  
18 cyclooctynes these reactions proceed slower than common CuAAC reactions. While we were  
19 working on this project, the groups of Huber<sup>45</sup> and Heemstra<sup>46</sup> independently presented strategies  
20 to increase the rate of SPAAC reactions by adding surfactants for the formation of micelles as  
21 confined compartments for the reaction to take place at high concentration. This strategy has  
22 recently been greatly advanced by the group of Lipshutz by applying novel designer surfactants  
23 for the acceleration of diverse transformations in water, such as Heck reactions, metal-catalyzed  
24 cross couplings, olefin metathesis and 1,4-addition of cuprates to enones.<sup>47-49</sup> Huber and  
25 coworkers had noted that azide residues of unnatural amino acids pointing into a hydrophobic  
26 pocket of a protein were more readily labeled by Alexa488-DIBO than those exposed to the  
27 aqueous environment. The authors thus deduced that the high hydrophobicity of the cyclooctyne  
28 substrates prevents them to react efficiently in SPAAC reactions in aqueous media and that the  
29 local environment at the site of reaction within the protein has a major effect on the rate of the  
30 SPAAC. By solubilizing the GPC receptors in their study with detergent (*n*-dodecyl  $\beta$ -D-  
31 maltoside), they observed a rate enhancement of up to a factor of 1000 compared to SPAAC  
32 reactions with azide groups on water-exposed surfaces. Heemstra and coworkers used the  
33 strongly hydrophobic DIBAC derivative to investigate its SPAAC reaction with a a) hydrophobic  
34 and b) hydrophilic (PEGylated) azide employing i) neutral (Tween, Triton X-100), ii) cationic

1  
2  
3 (DTAB, CTAB) and iii) anionic (SDS) surfactant additives using absorbance UV spectroscopy  
4  
5 for the determination of reaction rate constants. In conclusion, they found that rate enhancement  
6  
7 with the hydrophobic azide is much more pronounced and especially strong with cationic  
8  
9 surfactants (by a factor of 179). Recently, the Heemstra group has also systematically  
10  
11 investigated the effect of buffer identity (NaPi, Tris, TBE, MES, MOPS, HEPES, acetate), ionic  
12  
13 strength (by addition of NaCl) and organic cosolvents (DMSO, MeCN, NMP, MeOH, EtOH)  
14  
15 showing that moderate quantities of organic cosolvent lead to rate enhancement, whereas choice  
16  
17 of buffer and ionic strength has no substantial effect on the rate of reaction, as long as conditions  
18  
19 remain neutral.<sup>50</sup> Our goal was now to investigate SPAAC kinetics under a variety of reaction  
20  
21 conditions and buffer additives with special emphasis on pH. Such screening requires selection of  
22  
23 a suitable analytical method, which would allow for continuous monitoring of reaction progress  
24  
25 in combination with a wide range of conditions. This method needs to be applicable with  
26  
27 biological samples as well. Capillary zone electrophoresis does ideally fulfill these requirements.  
28  
29 It is a broadly applicable analytic method allowing for efficient separation of analytes with a wide  
30  
31 variety of compound classes ranging from small inorganic salts to complex biological samples.  
32  
33 Quantitative determination of physical chemical parameters of various compounds as well as  
34  
35 investigation of reaction kinetics by capillary electrophoresis has been shown to proceed with  
36  
37 high reliability.<sup>51-58</sup> This method does also offer deep insights into the separation process, as  
38  
39 electromigration is very well described with a solid theoretical foundation. The complete  
40  
41 mathematical model was implemented in several simulation programs, thus enabling optimization  
42  
43 of separation conditions and detailed planning of experiments.<sup>59-62</sup> Another advantage is the  
44  
45 method's versatility, as separation/reaction conditions are widely variable.  
46  
47  
48  
49  
50  
51  
52  
53

54 In this study, we use capillary electrophoresis as the method of choice for monitoring the  
55  
56 progress of SPAAC reactions under various reaction conditions to optimize the reaction by  
57

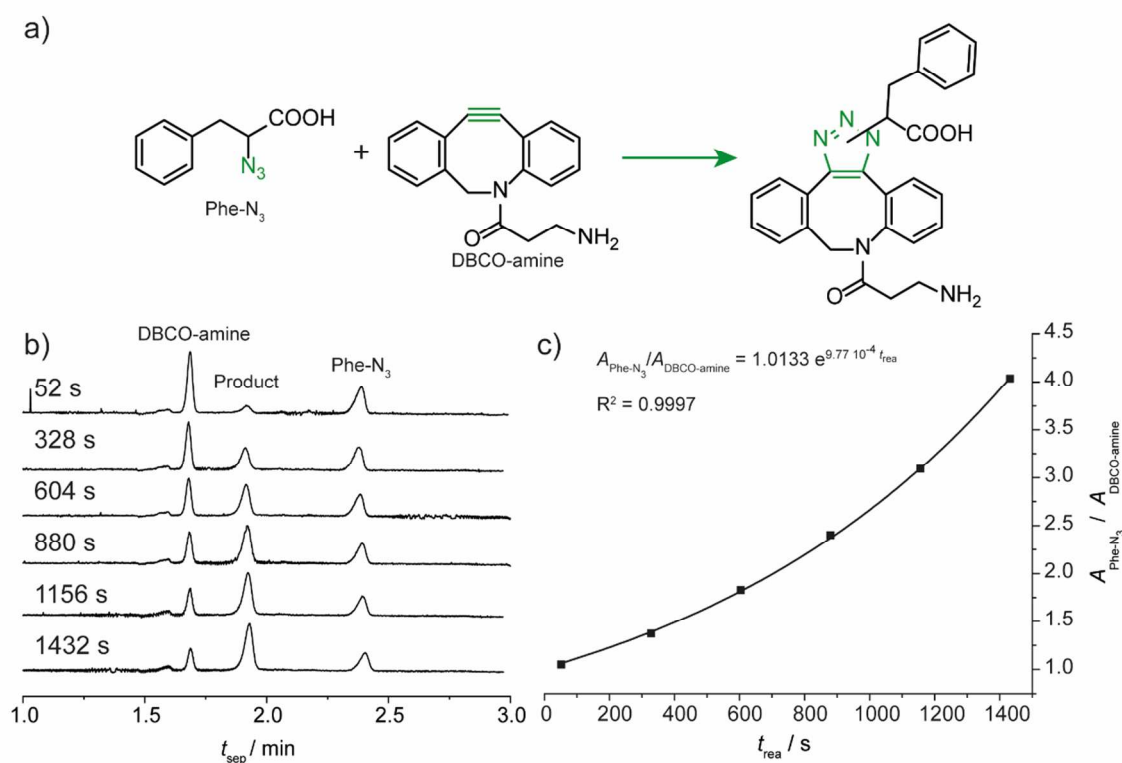
1  
2  
3 significant reaction rate enhancement. In a series of test reactions, cycloadditions of  
4 dibenzocyclooctyne-amine (3-amino-1-(11,12-didehydrodibenzo[*b,f*]azocin-5(6*H*)-yl)propan-1-  
5 one, DBCO-amine) with several azides were investigated. Systematically screening the reaction  
6 medium's pH, we observed clear trends regarding the dependence of the reaction rate on the  
7 charge state of the various azide substrates with acidic/basic substituents as well as on the charge  
8 state of DBCO-amine. Plausible structural scenarios were identified by DFT calculations. Next,  
9 the knowledge gained by our study varying the pH of the reaction medium was applied in  
10 reactions with surfactant additives. Due to the large rate enhancement, we propose the addition of  
11 surfactants to achieve efficient and fast SPAAC reactions in aqueous solution.  
12  
13  
14  
15  
16  
17  
18  
19  
20  
21  
22  
23  
24  
25  
26

## 27 **Results and Discussion**

28  
29  
30 Capillary electrophoresis was utilized for precise and fast determination of reaction kinetics. This  
31 novel electrophoretic method allows for continuous monitoring of the reaction mixture's  
32 composition. A suitable separation buffer was selected in order to provide baseline-separated  
33 symmetrical peaks of reactants and products, which do not coincide with any system peaks. The  
34 buffer composition was optimized under the premise that all reactants were soluble within a wide  
35 range of concentrations. PeakMaster 5.3 was utilized for optimization of separation  
36 conditions.<sup>61,62</sup> After careful optimization of the buffer composition for the different reaction  
37 mixtures, 7 mM  $\beta$ -alanine/10 mM LiOH buffer with 20 mM SDS (pH 11.45) and 28 vol% of  
38 acetonitrile was chosen for reactions with 4-azidophenol (PhOH-N<sub>3</sub>), 4-azidobenzene sulfonic  
39 acid (PhSO<sub>3</sub>H-N<sub>3</sub>), azidobenzoic acid (PhCOOH-N<sub>3</sub>), or (*S*)-2-azido-3-phenylpropionic acid  
40 (Phe-N<sub>3</sub>) as substrate, and a buffer composition of 15 mM citric acid/10 mM LiOH buffer with 15  
41 mM SDS (pH 3.34) was used in reactions with azidobenzene (Ph-N<sub>3</sub>). With these buffers all  
42  
43  
44  
45  
46  
47  
48  
49  
50  
51  
52  
53  
54  
55  
56  
57  
58  
59  
60

reactants were soluble up to a concentration of 10 mM. The cycloaddition products of DBCO with a variety of azides have already been investigated and resulting triazoles have been characterized.<sup>63,64</sup>

Our CE method was optimized for fast and effective separation of reactants and products covering a wide range of reaction rates ( $10^{-3}$ – $10^2$   $\text{dm}^3\text{mol}^{-1}\text{s}^{-1}$ ). Advantageously, neither internal standard nor calibration was necessary for data evaluation, as the ratio of the peak areas (and not the absolute values) were needed for kinetic evaluation (see Supporting Information, Section 1, equation 4). The CE method employed was tested by using simulation tool Simul 5 Complex-Kinetic,<sup>59,60</sup> which allowed us to computationally check the applicability of our method over a wide range of reaction rates (Supporting Information, Section S1). An illustrative sequence of electropherograms for one reaction and the resulting evaluation of the observed peak area ratios is depicted in Figure 1.



1  
2  
3 **Figure 1** A) Reaction scheme for SPAAC of Phe-N<sub>3</sub> with DBCO-amine. B) Electropherograms  
4 of the reaction mixture of Phe-N<sub>3</sub> and DBCO-amine at different reaction times with 20 mM SDS  
5 (for pH 6.59 at the start of the reaction). C) Evaluation of the electropherograms, plot of  
6  $A_{\text{Phe-N}_3}/A_{\text{DBCO-amine}}$  over time, black solid line: exponential fit. For residual plot of the exponential  
7 fit see Figure SI-3.  
8  
9  
10  
11

12 We focused mainly on the selection of a suitable reaction buffer regarding pH and choice of  
13 additives, as changing reaction conditions is the most efficient and time-saving way of optimizing  
14 reaction rates, for example in comparison to structural modifications on the substrate  
15 cyclooctynes. The reaction was optimized for commercially available DBCO-amine. The azides  
16 were chosen in a way to include functional groups with electron donating and withdrawing  
17 effects featuring acidic and basic functionalities that can be protonated/deprotonated depending  
18 on the pH of the reaction mixture. The substrates are shown in Figure 2b.  
19  
20  
21  
22  
23  
24  
25  
26  
27

28 First, we put our focus on the influence of buffer pH on the rate of SPAAC reaction. The  $pK_a$   
29 values of individual reactants were determined by capillary zone electrophoresis (for details see  
30 Supporting Information, Section S3), the resulting values are depicted in Figure 2b (azides) and  
31 2c (DBCO-amine). Figure 2a shows the plot of the reactants' effective charge (ordinate) in  
32 dependence on the reaction mixture's pH (abscissa) (PhSO<sub>3</sub><sup>-</sup>-N<sub>3</sub> is fully negatively charged and  
33 Ph-N<sub>3</sub> is neutral along the complete pH range). Based on these data, we were able to select  
34 suitable buffers covering the pH regions of various charge states of individual reactants (pH 2.29,  
35 3.77, 7.09, 11.55). The exact composition of buffers is given in the Supporting Information  
36 (Table SI-2).  
37  
38  
39  
40  
41  
42  
43  
44  
45  
46  
47  
48  
49  
50  
51  
52  
53  
54  
55  
56  
57  
58  
59  
60

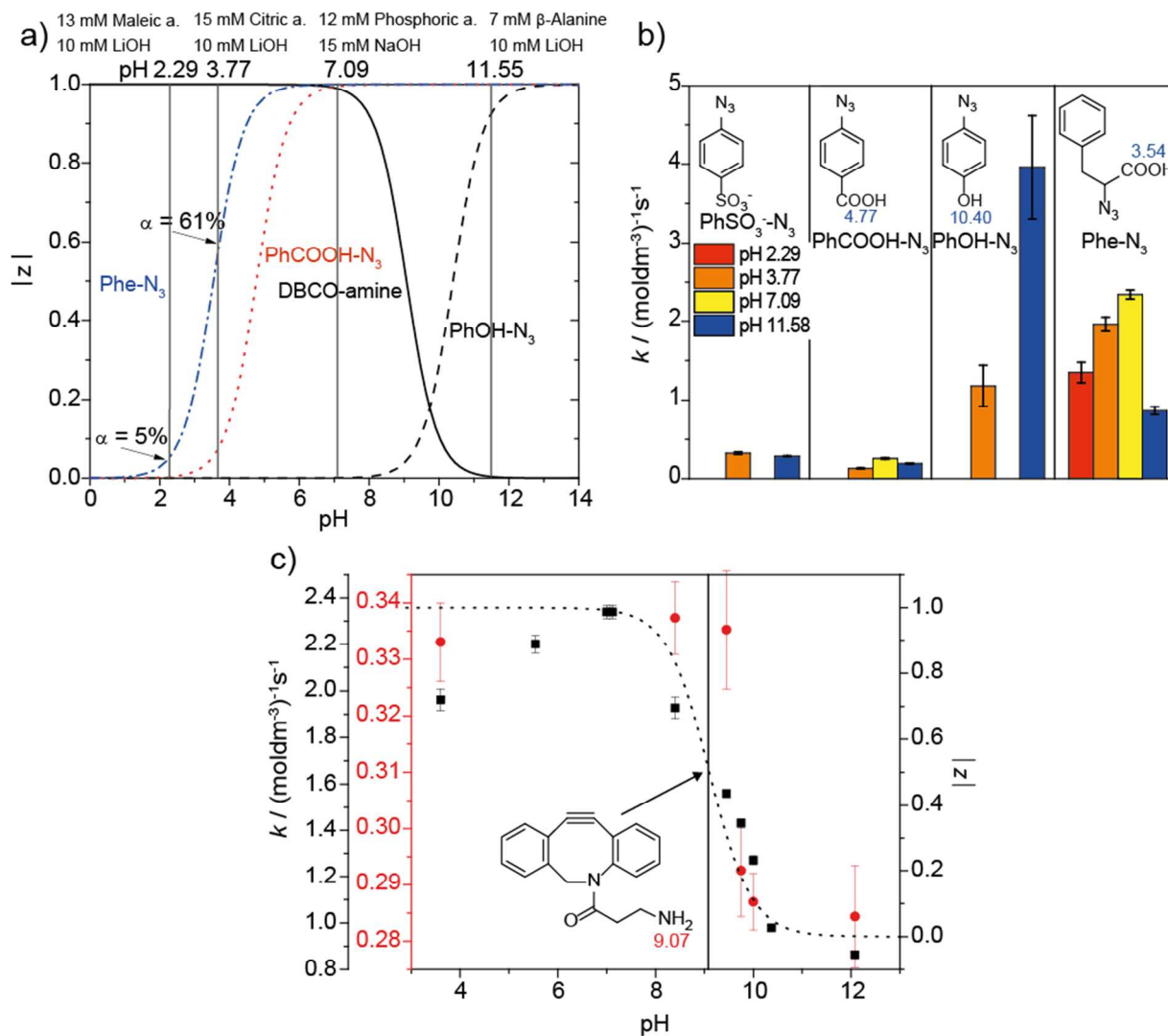


**Figure 2** (a) Effective charge ( $|z|$ ) of the reactants in dependence on the buffer's pH; black solid line: DBCO-amine; black dashed line: PhOH-N<sub>3</sub>; red dotted line: PhCOOH-N<sub>3</sub>; blue dot-dashed line: Phe-N<sub>3</sub>; the vertical lines represent individual buffer pH values, the composition of the corresponding buffer is given above each line. (b) Rate constants obtained for different azide substrates at various reaction buffer pH values, experimentally determined  $pK_a$  values for individual molecules are given in blue next to the respective acidic or basic functional group. (c) Rate constant  $k$  (left axis) of the SPAAC in dependence on the pH of the reaction buffer; black squares: Phe-N<sub>3</sub>; red dots: PhSO<sub>3</sub><sup>-</sup>-N<sub>3</sub>; dashed black line: effective charge ( $|z|$ ) of DBCO-amine (right axis).  $pK_a$  of DBCO-amine is depicted as a vertical line.

In the case of neutral Ph-N<sub>3</sub> and negatively charged sulfonate PhSO<sub>3</sub><sup>-</sup>-N<sub>3</sub>, the reaction was performed at pH 11.55 and pH 3.77, where the DBCO-amine is neutral and positively charged, respectively. The same conditions also applied for the reaction of PhOH-N<sub>3</sub> as the  $pK_a$  values of

1  
2  
3 PhOH-N<sub>3</sub> and DBCO-amine are very close (10.40 and 9.07, respectively). In the case of  
4  
5 PhCOOH-N<sub>3</sub> and Phe-N<sub>3</sub>, measurements were additionally performed at pH 7.09, where both  
6  
7 DBCO-amine and the azides' carboxylic acid groups in the side chain are charged.  
8  
9

10 As Phe-N<sub>3</sub> is a moderately strong acid (pK<sub>a</sub> 3.54), it is mainly dissociated ( $\alpha = 61\%$ ) in the citric  
11  
12 buffer solution (pH 3.77). For this reason, the rate of the SPAAC reaction with Phe-N<sub>3</sub> as  
13  
14 substrate was also measured in maleic acid buffer at pH 2.29, where the degree of dissociation is  
15  
16 about 5% (Figure 2a).  
17  
18  
19  
20  
21  
22

23 The determined reaction rates are summarized in Figure 2b. The highest reaction rates were  
24  
25 observed for PhOH-N<sub>3</sub>, which can be explained by the highly electron donating hydroxyl group.  
26  
27 This effect is even more pronounced for the deprotonated azidophenol (PhO<sup>-</sup>-N<sub>3</sub>). With  
28  
29 increasing pH value and the resulting deprotonation to the respective phenolate, the reaction rate  
30  
31 of the SPAAC with DBCO-amine increases by a factor of 3.4. In comparison, the reaction rates  
32  
33 of PhCOOH-N<sub>3</sub> and PhSO<sub>3</sub><sup>-</sup>-N<sub>3</sub> are significantly lower, which correlates well with the electron  
34  
35 withdrawing effect of the substituent. The unsubstituted azidobenzene (Ph-N<sub>3</sub>) is highly volatile  
36  
37 and its concentration decreases in the course of the reaction. Figure SI-4 shows the dependence of  
38  
39 the relative area of the Ph-N<sub>3</sub> peak on time, which proves that the concentration of azide  
40  
41 decreases in the same extent independently on the composition of the buffer used. No effect of  
42  
43 pH on the reaction rate of Ph-N<sub>3</sub> was observed.  
44  
45  
46  
47  
48

49 Obviously, the reaction rates observed for SPAAC reactions with Phe-N<sub>3</sub> increase with pH in  
50  
51 acidic pH regions, which can be explained by deprotonation of the carboxyl group as the medium  
52  
53 becomes more alkaline. In contrast to COOH, the carboxylate COO<sup>-</sup> is characterized by a much  
54  
55 attenuated electron-withdrawing effect. Surprisingly, the reaction rate is lower at basic  
56  
57  
58  
59  
60

1  
2  
3 conditions. The same trend is observed for all azides (except for PhOH-N<sub>3</sub>, where the effect of  
4 OH deprotonation to the phenolate PhO<sup>-</sup>-N<sub>3</sub> predominates). Figure 2c shows in detail the reaction  
5 rate's dependence on pH for these azide substrates. Clearly, for both Phe-N<sub>3</sub> and PhSO<sub>3</sub><sup>-</sup>-N<sub>3</sub>  
6 substrates, we observe the same drop in SPAAC reaction rate in the pH range 8–10. This is  
7 highly surprising as the charge state of neither PhSO<sub>3</sub><sup>-</sup>-N<sub>3</sub> nor Phe-N<sub>3</sub> changes in this pH region.  
8 This leads to the conclusion that deprotonation of the DBCO-ammonium ion in this pH regime  
9 has significant impact on the SPAAC reaction rate, independent on the structural characteristics  
10 of the azide reaction partner, which is further supported by the fact that the inflection point of the  
11 resulting curve corresponds very well with the pK<sub>a</sub> of DBCO-amine (Figure 2c). This result was  
12 surprising because of the large distance of the amino group as the site of protonation from the  
13 reactive triple bond of DBCO.  
14  
15  
16  
17  
18  
19  
20  
21  
22  
23  
24  
25  
26  
27  
28

29 Thermodynamic parameters of the SPAAC reaction of Phe-N<sub>3</sub> and DBCO-amine were  
30 determined experimentally in order to characterize the influence of the effective charge of  
31 DBCO-amine on the rate of reaction. The rate constants were determined at various temperatures  
32 (15, 20, 25, 30 and 40°C) in acidic and basic media. The corresponding Eyring plots and  
33 thermodynamic parameters are shown in Figure 3. The Gibbs energy was calculated at 20 °C,  
34 which gave values of  $\Delta G_N^\ddagger = 71.5 \pm 0.1 \text{ kJ mol}^{-1}$  and  $\Delta G_C^\ddagger = 70.0 \pm 0.4 \text{ kJ mol}^{-1}$  for neutral DBCO-  
35 amine and DBCO-ammonium ion, respectively. Thus, the difference in activation energies of  
36 SPAAC reactions with (unprotonated) DBCO-amine and (protonated) DBCO-ammonium ion is  
37  $1.6 \pm 0.5 \text{ kJ mol}^{-1}$  with the ammonium ion featuring lower activation energy and higher rate of  
38 reaction.  
39  
40  
41  
42  
43  
44  
45  
46  
47  
48  
49  
50  
51  
52  
53  
54  
55  
56  
57  
58  
59  
60

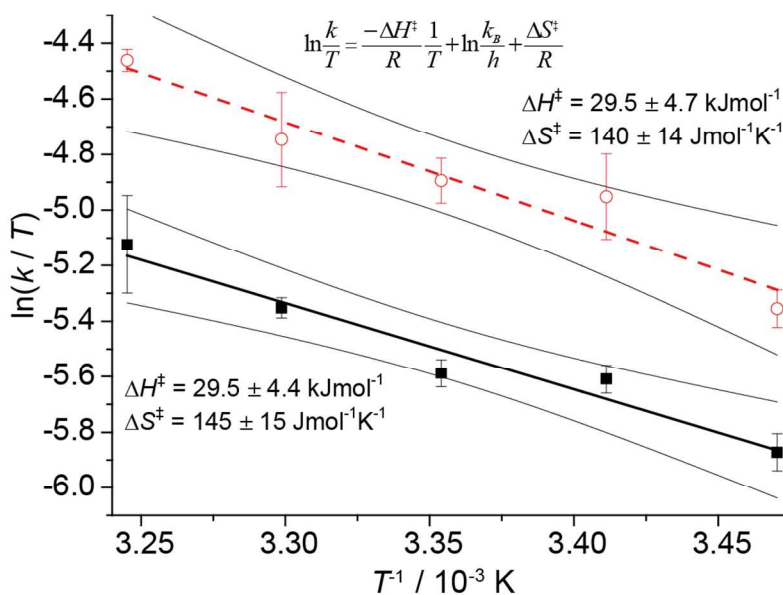


**Figure 3** Eyring analysis of the experimental rate constants of the SPAAC reaction with **Phe-N<sub>3</sub>** as determined by CE offline reaction. Solid squares: neutral DBCO-amine, transparent circles: protonated DBCO-amine (= DBCO ammonium ion). Errors are expressed as standard deviation; gray lines show the confidence interval on the 95 % level.

Inspired by the pioneering work of Bertozzi and Houk,<sup>34,35,44</sup> we subsequently investigated the SPAAC reaction by DFT calculations<sup>65,66</sup> with the aim of identifying different plausible reaction pathways that would rationalize the rate constant's pH dependence. We were aware of the small energy differences of the corresponding transition states and, therefore, we did not attempt to pinpoint one single favored mechanism, but rather screen possible trajectories thoroughly. All calculations were performed with Gaussian09 Rev.-D.01<sup>67</sup> on a B3LYP<sup>68-70</sup>/cc-pVDZ<sup>71-73</sup> level of theory including the D3 version of Grimme's dispersion correction.<sup>74</sup> Augmented basis sets (aug-cc-pVDZ) were used for all atoms involved in bond formation and hydrogen bonding interactions and a CPCM solvent model (acetonitrile unless otherwise specified) was applied.<sup>75,76</sup>

The focus of our theoretical investigations was the reaction of DBCO-amine with Phe-N<sub>3</sub> in acetonitrile. We initially performed a detailed geometry analysis of all possible conformers of DBCO-amine that arise due to the flexible  $\beta$ -alanine amide side chain in order to determine the

1  
2  
3 ground states of the reaction participants. Both in the protonated and in the non-protonated case,  
4 the amide bond *E*-configuration was found to be energetically favored. In the protonated state,  
5 there was a strong preference for conformers that allowed intramolecular hydrogen bonding  
6 interactions between the NH<sub>3</sub><sup>+</sup> group and the amide carbonyl (see Supporting Information,  
7 Section 4 for details).  
8  
9

10 We investigated the transition states considering protonated as well as non-protonated forms of  
11 the β-alanine side chain as well as the formation of both triazole regioisomers (DBCO-amine-11  
12 and DBCO-amine-12). We realized that the approach of the phenyl azide (Ph-N<sub>3</sub>) might either be  
13 of *syn* or *anti* orientation with respect to the β-alanine group. In the non-protonated state, both *syn*  
14 approaches also featured weak hydrogen bonding interactions of the NH<sub>2</sub> group and two azide  
15 nitrogen atoms. Additionally, we calculated one trajectory of an *anti* approach. The energy levels  
16  $\Delta\{E+ZPE\}$  and  $\Delta G^\ddagger(298\text{ K})$  of the three transition states were found to be quite similar  
17 (Figure 4a). We also identified three *syn* and one *anti* transition state for the protonated β-alanine  
18 side chain, some of them featuring hydrogen bonding interactions with the approaching azide.  
19 These transition states were found to be energetically comparable to those of the non-protonated  
20 analogues (Figure 4b).  
21  
22  
23  
24  
25  
26  
27  
28  
29  
30  
31  
32  
33  
34  
35  
36  
37  
38  
39  
40  
41  
42  
43  
44  
45  
46  
47  
48  
49  
50  
51  
52  
53  
54  
55  
56  
57  
58  
59  
60

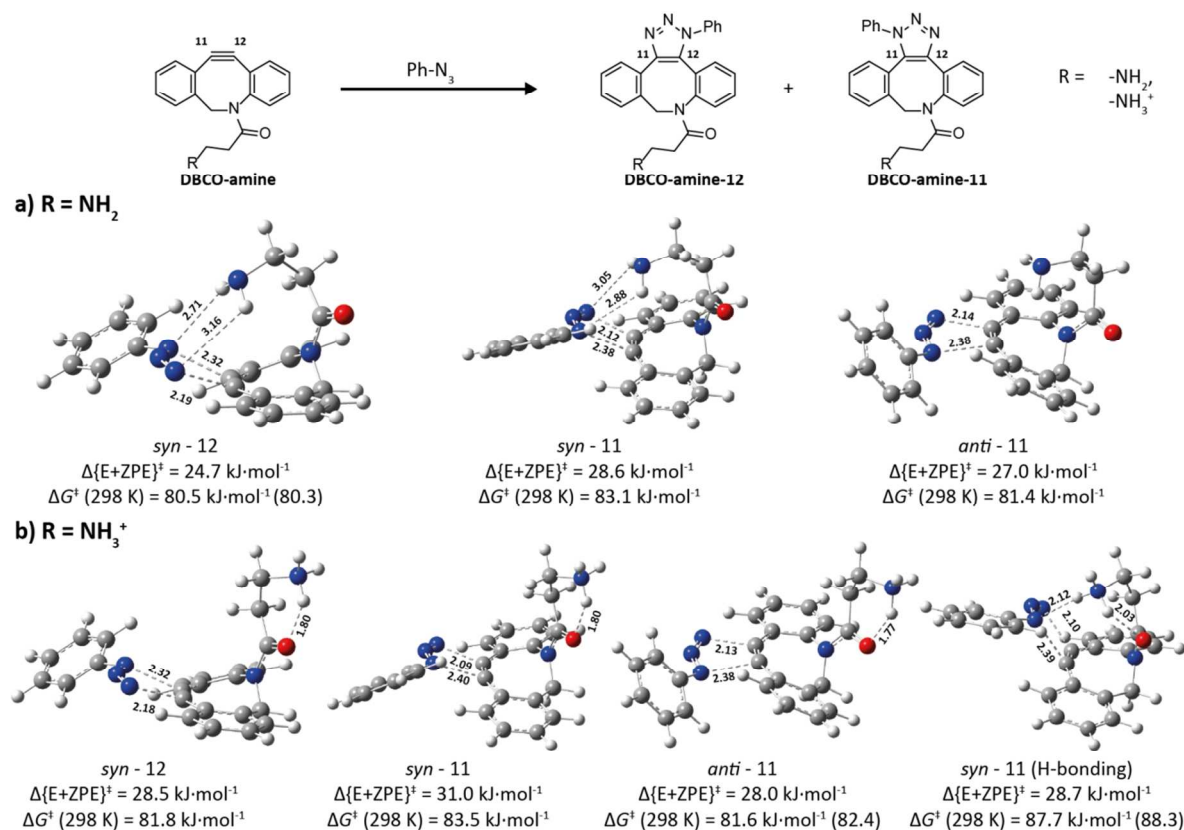


**Figure 4** DFT study of the reaction of strained DBCO-amine with Ph-N<sub>3</sub>. The transition state structures of the non-protonated (a) and protonated  $\beta$ -alanine side chain (b) are depicted together with the respective energy levels. Energy levels given in parentheses are results from calculations applying the CPCM solvent model for water (instead of MeCN). DFT calculations were performed at the B3LYP/cc-pVDZ level of theory including the D3 version of Grimme's dispersion correction. Augmented basis sets (aug-cc-pVDZ) were used for all atoms involved in bond formation and hydrogen bonding interactions and a CPCM solvent model was applied.

Detailed inspection of the transition state structures revealed that the protonation state of the  $\beta$ -alanine side chain might indeed affect the transition state energy. This might either be due to non-covalent interactions with the incoming azide molecule or due to subtle changes in electronic properties, which both can easily cause changes in the range of 1–2 kJ mol<sup>-1</sup>, which would match the differences in the experimentally observed rate constants of protonated and unprotonated DBCO-amine in SPAAC reactions.

1  
2  
3 In the next step, we extended our study to the SPAAC reaction with methyl azide in order to  
4 identify potential differences when an aliphatic azide takes part in the reaction. We identified two  
5 transition states (protonated and non-protonated  $\beta$ -alanine side chain) for the formation of each of  
6 the two possible regioisomers (Figure SI-6). Interestingly, the resulting transition state energies  
7 of  $\Delta\{E+ZPE\} = 26.0\text{--}28.5 \text{ kJ mol}^{-1}$  and  $\Delta G^\ddagger(298 \text{ K}) = 80.7\text{--}81.7 \text{ kJ mol}^{-1}$  are very similar to  
8 those with phenyl azide (Ph-N<sub>3</sub>) as reactant.  
9

10  
11  
12 All calculated transition state Gibbs energies seem to be systematically overestimated when  
13 compared to the experimental results. This is in agreement with the studies by Bertozzi and Houk  
14 *et al.*, who reported the B3LYP functional to result in overestimations of about  $27 \text{ kJ mol}^{-1}$  for  
15 calculations of SPAAC reactions.<sup>44,77</sup>  
16

17  
18 Summarizing this part of the study, we have determined the rate constants of SPAAC reactions at  
19 various pH values of different MeCN/water reaction media by continuous reaction monitoring  
20 with capillary electrophoresis. We have shown that the composition of the buffered reaction  
21 medium can significantly influence the reaction rate of the SPAAC reaction. Our study points to  
22 the necessity to always optimize SPAAC reaction conditions for a specific set of reactants with  
23 regard to the choice of buffer and pH, and introduces a versatile and powerful method to do so  
24 (e.g. in comparison to the much more tedious tuning of the reactants' structural characteristics). A  
25 strong influence on the rate of the SPAAC reaction was observed for different protonation states  
26 of the functionalized acidic or basic azides as well as for our test cycloalkyne substrate DBCO-  
27 amine. DFT calculations illustrate the manifold transition state geometries similar in energy that  
28 can be identified depending on the substrate's protonation state, and support our experimental  
29 findings.  
30  
31  
32  
33  
34  
35  
36  
37  
38  
39  
40  
41  
42  
43  
44  
45  
46  
47  
48  
49  
50  
51  
52  
53  
54  
55  
56  
57  
58  
59  
60

### **Influence of SDS micelles on the rate of the SPAAC reaction**

Sodium dodecyl sulfate (SDS) micelles can have an advantageous effect on the rate of reactions featuring highly hydrophobic compounds in polar reaction media, as has recently been reported for SPAAC reactions by the groups of Heemstra and Huber<sup>45,46</sup>. This effect is based on the incorporation of the hydrophobic reactants into the SDS micelles, which results in an increase in the reactants' local concentration and thus an enhancement of the rate of reaction.

At first, the interaction of all reactants with SDS micelles was characterized by capillary zone electrophoresis (CZE; Figure SI-7). Recently, we showed that SDS micelles can even be formed in media containing high concentrations of MeCN, with the critical micelle concentration (CMC) being only slightly shifted to higher concentrations of SDS.<sup>78</sup> To characterize the micellization in our particular solvent mixture (28 vol% MeCN in water), we determined the CMC of SDS by fluorescence correlation spectroscopy (FCS) as well as mobility measurements (see Figure SI-8A and SI-8B for details). The resulting value of CMC in the water/MeCN mixture (28 vol% MeCN) is 13 mM. Simultaneously, the mobility of all reactants was measured in dependence on the SDS concentration (Figure 5 and SI-7). Based on these data two concentrations above the CMC, 20 mM and 50 mM SDS, were chosen for investigations of the SPAAC reaction kinetics.

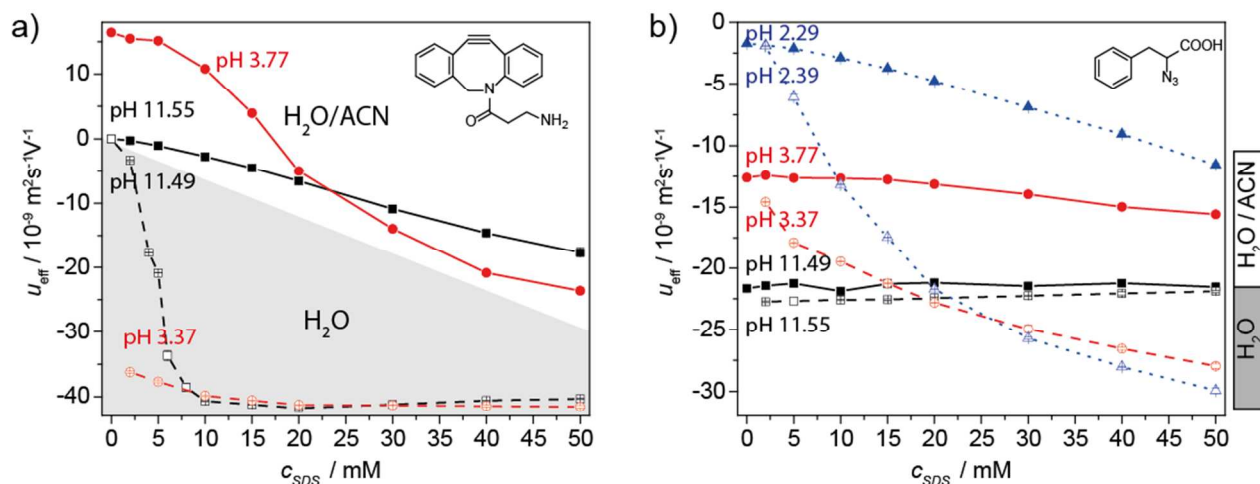


**Figure 5** Effective mobility of the reactants in dependence on the concentration of SDS in the background electrolyte (BGE). a) DBCO-amine, b) Phe-N<sub>3</sub>. Solid squares pH 11.55 (MeCN/H<sub>2</sub>O, pH at SDS 0 mM), transparent squares pH 11.49 (H<sub>2</sub>O, pH at SDS 0 mM); solid circles pH 3.77 (MeCN/H<sub>2</sub>O, pH at SDS 0 mM), transparent circles 3.37 (H<sub>2</sub>O, pH SDS 0 mM), solid triangles pH 2.29 (MeCN/H<sub>2</sub>O, SDS 0 mM), transparent triangles pH 2.39 (H<sub>2</sub>O, pH SDS 0 mM), transparent symbols: measurements in aqueous buffers, solid symbols: in H<sub>2</sub>O/MeCN buffer. For pH values at different SDS concentration see Table SI-1. Errors are expressed as standard deviations.

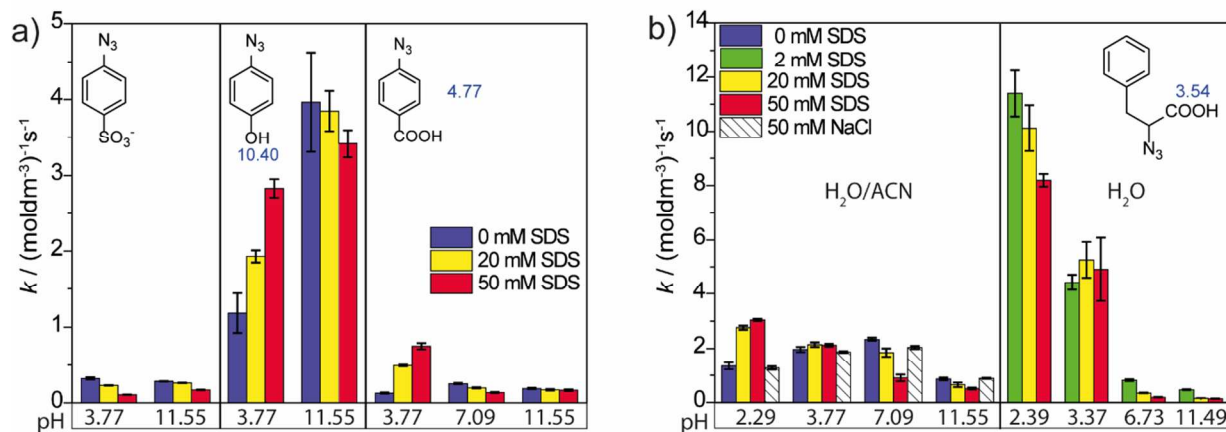


**Figure 6** (a) Rate constants of SPAAC reactions with various azides and DBCO-amine in dependence on pH and concentration of SDS. (b) Rate constant of reaction of Phe-N<sub>3</sub> with DBCO-amine depending on concentrations of SDS, pH and concentration of NaCl. Buffer solutions containing 28 vol% MeCN labeled MeCN/H<sub>2</sub>O and aqueous buffers labeled H<sub>2</sub>O. Errors are given as standard deviations. For pH values at different SDS concentration see Table SI-1.

1  
2  
3 Based on these findings, the reaction kinetics was investigated at 0 mM, 20 mM and 50 mM  
4 SDS. The reaction rate of Ph-N<sub>3</sub> increases with addition of SDS independently on the pH value of  
5 the reaction medium. We attribute this effect to the strong interaction of both Ph-N<sub>3</sub> and DBCO-  
6 amine with SDS micelles. On the other hand, PhSO<sub>3</sub><sup>-</sup>-N<sub>3</sub> is very hydrophilic, which disfavors its  
7 incorporation in micelles, which results in a decrease in the reaction rate after addition of SDS at  
8 both acidic and basic pH (Figure 6a), because the azide concentration is lowered in the micelle  
9 under these conditions.  
10  
11

12  
13  
14  
15  
16  
17  
18  
19  
20 PhOH-N<sub>3</sub>'s pK<sub>a</sub> is in a similar range as the pK<sub>a</sub> of protonated DBCO-amine, which means that in  
21 acidic pH the phenol moiety of PhOH-N<sub>3</sub> is not deprotonated, while DBCO-amine is fully  
22 protonated (ammonium ion). From the observed rate enhancement of the SPAAC reaction, we  
23 derive that both compounds interact strongly with SDS, which results in significant increase of  
24 rate constants. The opposite effect can be observed at basic pH, where PhOH-N<sub>3</sub> is negatively  
25 charged upon deprotonation of the phenol and DBCO-amine is not protonated and neutral.  
26  
27  
28  
29  
30  
31  
32  
33

34  
35 Higher concentrations of SDS lead to an increase in the rate constants of SPAAC reactions with  
36 PhCOOH-N<sub>3</sub> at acidic pH, where the azide's carboxylic acid group is not deprotonated (neutral)  
37 and DBCO-amine protonated (cationic) both interacting strongly with micelles. On the other  
38 hand, at pH 11.55 PhCOOH-N<sub>3</sub> is fully dissociated and avoids the micelle environment, which  
39 results in a decrease of reaction rate. This effect is even more pronounced at pH 7.09, where  
40 DBCO-amine is cationic and interacts with SDS significantly (see Figure 6a). Very similar  
41 behavior was observed for Phe-N<sub>3</sub>. The largest rate enhancement was observed at pH 2.29, where  
42 the azide reactant Phe-N<sub>3</sub> interacts strongest with SDS. At pH 3.77 almost no effect of SDS  
43 addition was observed, as Phe-N<sub>3</sub> is mainly dissociated ( $\alpha = 60\%$  at pH 3.77). Similarly to  
44  
45  
46  
47  
48  
49  
50  
51  
52  
53  
54  
55  
56  
57  
58  
59  
60

1  
2  
3 PhCOOH-N<sub>3</sub>, the decrease of the reaction rate is evident at pH 11.55 and most pronounced at pH  
4  
5 7.09.  
6  
7  
8  
9

10  
11 We have to point out that addition of SDS results in simultaneous increase of ionic strength,  
12  
13 which can result in changes of reaction kinetics. By increasing the ionic strength, the reaction rate  
14  
15 can either increase or decrease depending on the effective charges of reactants according to the  
16  
17 following equation  
18  
19

$$20 \log k = \log k^0 + 1.02 z_A z_B \sqrt{I}, \quad (1)$$

21  
22 where  $k^0$  is the rate constant at infinite dilution,  $z_A$  and  $z_B$  are the effective charges of reactants,  $I$   
23  
24 is ionic strength. It means that for reactants of opposite charge the rate constant decreases with  
25  
26 increasing ionic strength and vice versa. If one of the reactants is neutral, no effect of the ionic  
27  
28 strength on rate constants can be observed.  
29  
30  
31  
32  
33

34  
35 Our reactants are always of opposite charge or at least one of them is neutral, so the rate constants  
36  
37 should either decrease with ionic strength or be independent of ionic strength, respectively.  
38  
39 These theoretical predictions were experimentally confirmed for SPAAC reactions with Phe-N<sub>3</sub>.  
40  
41 The rate constants were determined at higher ionic strength by addition of 50 mM NaCl to the  
42  
43 SPAAC reaction mixture. The experimental results are summarized in Figure 6b. At highly acidic  
44  
45 or basic pH, where either the functionalized azide or DBCO-amine is neutral, the effect of ionic  
46  
47 strength on the reaction kinetics is negligible. A very slight decrease of rate constants was  
48  
49 observed at pH 3.77, where Phe-N<sub>3</sub> is partially dissociated. At pH 7.09, where both reactants are  
50  
51 charged, the decrease of SPAAC reaction rate is the most remarkable. At this pH, the rate  
52  
53 constants were determined also at 20 mM concentration of NaCl to be able to compare the effect  
54  
55  
56  
57  
58  
59  
60

1  
2  
3 of ionic strength with the effect of SDS at the same concentration. Only a slight decrease of the  
4  
5 reaction rate was observed. Thus, we conclude that the effect of ionic strength on the rate  
6  
7 constants is negligible in comparison to the influence of adding SDS.  
8  
9

10 The major drawback of the SPAAC reaction is the poor solubility of cyclooctyne reactants in  
11  
12 water, which makes the use of MeCN/water mixtures for the reaction necessary. Acetonitrile is  
13  
14 toxic, which limits the applicability of SPAAC in biological applications. We have shown that  
15  
16 DBCO-amine interacts with SDS (*vide supra*), which indicates that addition of SDS should  
17  
18 improve the solubility of DBCO-amine in aqueous buffers. We were able to reach a solubility of  
19  
20 DBCO-amine of up to 5mM in 20 mM SDS solution. Similar improvement of solubility by  
21  
22 addition of SDS was observed also for neutral azides.  
23  
24  
25  
26

27 Thus, we were able to perform SPAAC reactions in purely aqueous reaction media. The reaction  
28  
29 was monitored for commercially obtained Phe-N<sub>3</sub>. Similarly to the previously described reactions  
30  
31 carried out in MeCN/H<sub>2</sub>O, the reactants' interactions with SDS were characterized by  
32  
33 electrophoretic measurements (Figure 5). DBCO-amine and the non-dissociated carboxylic acid  
34  
35 Phe-N<sub>3</sub> interact much stronger with micelles in aqueous environment than in MeCN/H<sub>2</sub>O buffer  
36  
37 solutions. Although the CMC of SDS determined at the same ionic strength is 5 mM, the  
38  
39 intensive interaction with SDS was observed already at much lower concentration (2 mM), which  
40  
41 is evident from its highly negative mobility (Figure 5a). Based on these results, we expect  
42  
43 significant improvement of the rate of the SPAAC reaction in acidic pH regions, while the  
44  
45 reaction at basic pH should be slowed down.  
46  
47  
48  
49  
50

51 The rate constants were determined at 2 mM, 20 mM and 50 mM concentrations of SDS, as  
52  
53 shown in Figure 6b. The rate constant observed at an SDS concentration of 2 mM (pH 2.39) is  
54  
55 11.4 dm<sup>3</sup>mol<sup>-1</sup>s<sup>-1</sup>, which is about ten times higher than in the MeCN/H<sub>2</sub>O mixture  
56  
57

1  
2  
3 (1.3 dm<sup>3</sup>mol<sup>-1</sup>s<sup>-1</sup>) under comparable conditions. The rate constants slightly decrease with  
4  
5 increasing concentration of SDS, as the maximum interaction between reactants and micelles is  
6  
7 already achieved at a concentration of 2 mM and addition of further micelles causes dilution of  
8  
9 the reactants in the micellar space. Also, we observed a very slight increase of pH after addition  
10  
11 of SDS under these conditions, possibly due to partial protonation of SDS ( $pK_a$  (sodium dodecyl  
12  
13 sulfonic acid) = 1) (Table SI-1).  
14  
15

16  
17 At pH 3.37 the rate constants are already lower (2 mM SDS, 4.4 dm<sup>3</sup>mol<sup>-1</sup>s<sup>-1</sup>), but still  
18  
19 significantly higher than in MeCN/H<sub>2</sub>O buffers in the absence of any surfactant. The rate  
20  
21 constants change with the SDS concentration only in the range of experimental error.  
22  
23

24  
25 At neutral and basic pH, the rate constants are much lower than in the acidic pH region or in  
26  
27 MeCN/H<sub>2</sub>O buffers without any surfactant. The rate of the reaction is highest at 2 mM SDS  
28  
29 concentration and decreases with increasing concentrations of SDS, as higher fractions of DBCO-  
30  
31 amine are incorporated in the micelles, while the azide is mostly found in the aqueous phase.  
32  
33

34  
35 Optimal results were achieved by combining the rate-enhancing effects of an adequate choice of  
36  
37 pH for the respective reactants and addition of a surfactant for micelle formation. Thus, the  
38  
39 reaction rate of the SPAAC reaction between Phe-N<sub>3</sub> and DBCO-amine can be accelerated by a  
40  
41 factor of up to 80 in the presence of 2 mM SDS in an aqueous buffer at pH 2.39. Thus, we  
42  
43 conclude that all reaction parameters need to be carefully optimized. The reaction rate constants  
44  
45 determined in our study range from three times lower up to ten times higher compared to rate  
46  
47 constants reported in literature for SPAAC reactions with similar azide substrates and under  
48  
49 comparable reaction conditions (see Table SI-6).<sup>50,79</sup>  
50  
51  
52  
53  
54  
55  
56  
57

## Conclusion

Our novel and user-friendly electrophoretic method allows for continuous, fast and reliable determination of the rate of reaction in SPAAC. The method is suitable for a wide range of reaction conditions. Thus, screening of various reaction conditions becomes feasible in a time-efficient manner. Screening parameters include the choice of buffer, buffer additives and the pH of the reaction medium. Having established this analytical method, we gained valuable insights for the optimization of SPAAC reaction conditions: we found that the charge state of functionalized azides containing either acidic or basic functional side chains has a major impact on the rate of the SPAAC reaction with test cyclooctyne DBCO-amine. These results were in good correlation with theoretical trends, which proved the high accuracy of our methods. As we found the charge state of cyclooctyne substrate DBCO-amine to also have an impact on the rate of reaction, we computationally calculated reaction trajectories featuring this cyclooctyne in different protonation states by DFT methods. Our results suggest that subtle changes in transition states, like hydrogen bonding interactions or minor changes in the electronic structure, account for the observed changes of rate constants. We also investigated the effect of SDS micelle formation on the rate of reaction, thus proving the power of the newly developed CE method. We observed substantial impact of SDS addition on the rate of SPAAC reaction with highly hydrophobic compounds. Carrying out the SPAAC reaction in micellar environment also allowed for running the reaction in a purely aqueous environment. Based on the proper selection of reaction conditions, the reaction rate was improved up to a factor of 80.

## Experimental Section

## Capillary Zone Electrophoresis

All electrophoretic experiments were performed on/with Agilent 3D<sup>CE</sup> capillary electrophoresis equipment operated under/by ChemStation software (Agilent Technologies, Waldbronn, Germany). Fused silica capillaries (50  $\mu\text{m}$  i.d., 375  $\mu\text{m}$  o.d.) were provided by MicroQuartz (Munich, Germany). The experiments were performed in bare fused silica capillaries with a total length and effective length to the diode array detector (DAD) of approximately 35.9 cm and 27.4 cm, respectively. New capillaries were flushed with H<sub>2</sub>O for 5 min, then for 5 min with 1M NaOH and for 10 min with H<sub>2</sub>O again. UV-detection was performed at wavelengths  $\lambda = 214$  nm and 230 nm, *i.e.* at the reactants' absorbance maxima.

The pH values were determined by a LAB 850 pH meter (SI Analytics, Lyon, France) calibrated with standard IUPAC buffers at pH 1.679, pH 7.000, pH 10.012 and pH 12.450.

Reaction kinetics was determined by means of CZE, the reaction was performed directly in sample vial. Reaction mixture was regularly injected to the system and analyzed. In addition to a 20 kV separation voltage, a hydrodynamic pressure of 50 mbar was applied during the measurements in order to increase the separation speed and allow for a short injection interval of about 3 min. The temperature of the cassette as well as the reaction vials was kept constant at 20°C.

The capillary was flushed with the separation buffer for 4 min before each sequence of measurements. The capillary was not flushed in between individual runs in order to shorten the time between injections. We did not observe any baseline deviations even after 15 injections.

The samples were injected hydrodynamically at 30 mbar $\times$ 5 s. Sample preparation was performed according to the following procedure: the stock solution of DBCO-amine was prepared in a

1  
2  
3 concentration of 10 mg/ml (36.2 mM) in acetonitrile (MeCN), due to its insolubility in water. The  
4  
5 same stock solution was used for all measurements. The stock solutions of azides at a mass  
6  
7 concentration of 10 mg/ml were prepared directly in the respective buffer.  
8

9  
10 The stock solutions of DBCO-amine and azides were further diluted by the reaction buffer  
11  
12 directly in the reaction vial. The concentration of DBCO-amine was 0.5 mM and the  
13  
14 concentration of azide varied between 0.6 mM to 1.5 mM depending on the reaction rate under  
15  
16 particular conditions and with the type of azide derivative used. Reactions were performed  
17  
18 directly in the electrophoretic vial with a total volume of 300  $\mu$ l.  
19

20  
21 Reaction kinetics was determined at various pH values in order to elucidate the effect of  
22  
23 dissociation of the reactants. The composition and pH of the buffers used in this study are  
24  
25 summarized in Table SI-1. Buffers contained 28 vol% of acetonitrile to ensure sufficient  
26  
27 solubility of the reactants.  
28

29  
30 The rate constants were also measured at 2mM, 20 mM and 50 mM concentrations of SDS and  
31  
32 after addition of 20 mM and 50 mM NaCl in the case of Phe-N<sub>3</sub>.  
33

34  
35 Kinetics of the cycloaddition of Phe-N<sub>3</sub> with DBCO-amine was also investigated in purely  
36  
37 aqueous reaction media *without* addition of MeCN in the presence of SDS. The rate of reaction  
38  
39 was measured at three concentrations of SDS: 2 mM, 20 mM and 50 mM. The composition of the  
40  
41 buffers was the same as in the case of MeCN/H<sub>2</sub>O buffers, see Table SI-1.  
42

43  
44 All measurements were performed in triplicates.  
45  
46  
47  
48

## 49 **Synthetic Procedures**

50  
51 Phenyl azide,<sup>80</sup> *p*-azidophenol<sup>81</sup> and *p*-azidobenzoic acid<sup>82</sup> were prepared according to literature  
52  
53 procedures. All spectroscopic data was in accordance with reported characterization.  
54  
55  
56  
57

**Synthesis of sodium *p*-azidobenzenesulfonate.**<sup>83</sup> This compound was prepared using a modified literature procedure.<sup>82</sup> An aqueous solution of NaNO<sub>2</sub> (497 mg, 7.22 mmol) was added dropwise to a solution of sulfanilic acid (1.00 g, 5.77 mmol) in 2 N hydrochloric acid (20 mL) under ice cooling. After an hour, an aqueous solution (3 mL) of sodium azide (2.00 equiv.) was added and stirred at room temperature for at least 15 hours. The solid sodium salt was formed by adding sodium chloride, separated by filtration and dried under reduced pressure. Sodium *p*-azidobenzenesulfonate was obtained in 56 % yield (711 mg, 3.21 mmol), including approximately 10 % sodium chloride according to elemental analysis. <sup>1</sup>H NMR (400 MHz, *d*<sub>6</sub>-DMSO) δ 7.64 (d, *J* = 8.5 Hz, 1H), 7.08 (d, *J* = 8.5 Hz, 1H) ppm; <sup>13</sup>C{<sup>1</sup>H} NMR (101 MHz, *d*<sub>6</sub>-DMSO) δ 145.0, 139.5, 127.5, 118.4 ppm; elemental analysis: calculated C – 32.58 %, H – 1.82 %, N – 19.00 %, S – 14.50 %, Na – 10.39 %, O – 21.70 %; found: C – 29.40 %, H – 1.91 %, N – 17.31 %, Cl – 7.82 %.

### DFT calculations

All computational results of this work were obtained by applying density functional theory methods (DFT)<sup>65,66</sup> using the Gaussian09 Revision-D.01 program package.<sup>67</sup> The B3LYP functional<sup>68,69</sup> has been used together with the cc-pVDZ basis set<sup>71,72</sup> for all structures. All geometries were optimized without symmetry restrictions and with the D3 version of Grimme's dispersion correction (gd3).<sup>74</sup> Solvation energy corrections were calculated using the CPCM model.<sup>75,76</sup> Transitions states were confirmed by occurrence of one, and only one, imaginary frequency in the Hesse matrix.

### Associated Content

The supporting information is available free of charge on the ACS Publication website. Experimental Procedures – Electrophoretic Methods – Synthetic Procedures – Computational Data with Optimized Ground State Geometries – Determination of Effective Mobilities and Critical Micelle Concentrations – NMR Spectra

1  
2  
3 **Notes**  
4

5 The authors declare no competing financial interest.  
6  
7

8 **Acknowledgements**  
9

10 J.S. thanks the Alexander von Humboldt Foundation for a postdoctoral fellowship and G.S.  
11 acknowledges the Fonds der Chemischen Industrie for a Ph.D. fellowship.  
12  
13  
14  
15  
16  
17  
18  
19  
20  
21  
22  
23  
24  
25  
26  
27  
28  
29  
30  
31  
32  
33  
34  
35  
36  
37  
38  
39  
40  
41  
42  
43  
44  
45  
46  
47  
48  
49  
50  
51  
52  
53  
54  
55  
56  
57  
58  
59  
60

## References

- (1) Kolb, H. C.; Finn, M. G.; Sharpless, K. B. *Angew. Chem. Int. Ed.* **2001**, *40*, 2004.
- (2) Rostovtsev, V. V.; Green, L. G.; Fokin, V. V.; Sharpless, K. B. *Angew. Chem. Int. Ed.* **2002**, *41*, 2596.
- (3) Hein, J. E.; Fokin, V. V. *Chem. Soc. Rev.* **2010**, *39*, 1302.
- (4) Huisgen, R. *Proc. Chem. Soc.* **1961**, 357.
- (5) Huisgen, R. *Angew. Chem. Int. Ed.* **1963**, *2*, 565.
- (6) Huisgen, R. *Angew. Chem. Int. Ed.* **1963**, *2*, 633.
- (7) Huisgen, R. *Pure Appl. Chem.* **1989**, *61*, 613.
- (8) R. Huisgen, *1,3-Dipolar Cycloaddition Chemistry*, Ed.: A. Padwa, Wiley, New York, **1984**.
- (9) Tornøe, C. W.; Christensen, C.; Meldal, M. *J. Org. Chem.* **2002**, *67*, 3057.
- (10) García-Álvarez, J.; Díez, J.; Gimeno, J.; Suárez, F. J.; Vincent, C. *Eur. J. Inorg. Chem.* **2012**, *2012*, 5854.
- (11) Gaulier, C.; Hospital, A.; Legeret, B.; Delmas, A. F.; Aucagne, V.; Cisnetti, F.; Gautier, A. *Chem. Commun.* **2012**, *48*, 4005.
- (12) Özçubukçu, S.; Ozkal, E.; Jimeno, C.; Pericàs, M. A. *Org. Lett.* **2009**, *11*, 4680.
- (13) Ahlquist, M.; Fokin, V. V. *Organometallics* **2007**, *26*, 4389.
- (14) Straub, B. F. *Chem. Commun.* **2007**, 3868.
- (15) Worrell, B. T.; Malik, J. A.; Fokin, V. V. *Science* **2013**, *340*, 457.
- (16) Berg, R.; Straub, B. F. *Beilstein J. Org. Chem.* **2013**, *9*, 2715.
- (17) Iacobucci, C.; Reale, S.; Gal, J.-F.; De Angelis, F. *Angew. Chem. Int. Ed.* **2015**, *54*, 3065.
- (18) Wang, Q.; Chan, T. R.; Hilgraf, R.; Fokin, V. V.; Sharpless, K. B.; Finn, M. G. *J. Am. Chem. Soc.* **2003**, *125*, 3192.
- (19) Speers, A. E.; Adam, G. C.; Cravatt, B. F. *J. Am. Chem. Soc.* **2003**, *125*, 4686.
- (20) Hein, C. D.; Liu, X.-M.; Wang, D. *Pharm. Res.* **2008**, *25*, 2216.
- (21) El-Sagheer, A. H.; Brown, T. *Chem. Soc. Rev.* **2010**, *39*, 1388.
- (22) Besanceney-Webler, C.; Jiang, H.; Zheng, T.; Feng, L.; Soriano del Amo, D.; Wang, W.; Klivansky, L. M.; Marlow, F. L.; Liu, Y.; Wu, P. *Angew. Chem. Int. Ed.* **2011**, *50*, 8051.
- (23) Thirumurugan, P.; Matosiuk, D.; Jozwiak, K. *Chem. Rev.* **2013**, *113*, 4905.
- (24) Yang, M.; Li, J.; Chen, P. R. *Chem. Soc. Rev.* **2014**, *43*, 6511.
- (25) Prescher, J. A.; Bertozzi, C. R. *Nat. Chem. Biol.* **2005**, *1*, 13.
- (26) Sletten, E. M.; Bertozzi, C. R. *Angew. Chem. Int. Ed.* **2009**, *48*, 6974.
- (27) Sletten, E. M.; Bertozzi, C. R. *Acc. Chem. Res.* **2011**, *44*, 666.
- (28) Brewer, G. J. *Chem. Res. Toxicol.* **2010**, *23*, 319.
- (29) Kennedy, D. C.; McKay, C. S.; Legault, M. C. B.; Danielson, D. C.; Blake, J. A.; Pegoraro, A. F.; Stollow, A.; Mester, Z.; Pezacki, J. P. *J. Am. Chem. Soc.* **2011**, *133*, 17993.
- (30) Agard, N. J.; Prescher, J. A.; Bertozzi, C. R. *J. Am. Chem. Soc.* **2004**, *126*, 15046.
- (31) Debets, M. F.; van Berkel, S. S.; Dommerholt, J.; Dirks, A. J.; Rutjes, F. P. J. T.; van Delft, F. L. *Acc. Chem. Res.* **2011**, *44*, 805.
- (32) Blomquist, A. T.; Liu, L. H. *J. Am. Chem. Soc.* **1953**, *75*, 2153.
- (33) Wittig, G.; Krebs, A. *Chem. Ber.* **1961**, *94*, 3260.
- (34) Ess, D. H.; Jones, G. O.; Houk, K. N. *Org. Lett.* **2008**, *10*, 1633.

- (35) Schoenebeck, F.; Ess, D. H.; Jones, G. O.; Houk, K. N. *J. Am. Chem. Soc.* **2009**, *131*, 8121.
- (36) Bach, R. D. *J. Am. Chem. Soc.* **2009**, *131*, 5233.
- (37) Agard, N. J.; Baskin, J. M.; Prescher, J. A.; Lo, A.; Bertozzi, C. R. *ACS Chem. Biol.* **2006**, *1*, 644.
- (38) Baskin, J. M.; Prescher, J. A.; Laughlin, S. T.; Agard, N. J.; Chang, P. V.; Miller, I. A.; Lo, A.; Codelli, J. A.; Bertozzi, C. R. *Proc. Natl. Acad. Sci.* **2007**, *104*, 16793.
- (39) Codelli, J. A.; Baskin, J. M.; Agard, N. J.; Bertozzi, C. R. *J. Am. Chem. Soc.* **2008**, *130*, 11486.
- (40) Ning, X.; Guo, J.; Wolfert, M. A.; Boons, G.-J. *Angew. Chem. Int. Ed.* **2008**, *47*, 2253.
- (41) Sletten, E. M.; Nakamura, H.; Jewett, J. C.; Bertozzi, C. R. *J. Am. Chem. Soc.* **2010**, *132*, 11799.
- (42) Debets, M. F.; van Berkel, S. S.; Schoffelen, S.; Rutjes, F. P. J. T.; van Hest, J. C. M.; van Delft, F. L. *Chem. Commun.* **2010**, 46, 97.
- (43) Jewett, J. C.; Sletten, E. M.; Bertozzi, C. R. *J. Am. Chem. Soc.* **2010**, *132*, 3688.
- (44) Gordon, C. G.; Mackey, J. L.; Jewett, J. C.; Sletten, E. M.; Houk, K. N.; Bertozzi, C. R. *J. Am. Chem. Soc.* **2012**, *134*, 9199.
- (45) Tian, H.; Sakmar, T. P.; Huber, T. *ChemBioChem* **2015**, *16*, 1314.
- (46) Anderton, G. I.; Bangerter, A. S.; Davis, T. C.; Feng, Z. Y.; Furtak, A. J.; Larsen, J. O.; Scroggin, T. L.; Heemstra, J. M. *Bioconjugate Chem.* **2015**, *26*, 1687.
- (47) Lipshutz, B. H.; Ghorai, S. *Aldrichimica Acta* **2008**, *41*, 59.
- (48) Lipshutz, B. H.; Ghorai, S. *Aldrichimica Acta* **2012**, *45*, 3.
- (49) Lipshutz, B. H.; Huang, S.; Leong, W. W. Y.; Isley, N. A. *J. Am. Chem. Soc.* **2012**, *134*, 19985.
- (50) Davis, D. L.; Price, E. K.; Aderibigbe, S. O.; Larkin, M. X. H.; Barlow, E. D.; Chen, R.; Ford, L. C.; Gray, Z. T.; Gren, S. H.; Jin, Y.; Keddington, K. S.; Kent, A. D.; Kim, D.; Lewis, A.; Marrouche, R. S.; O'Dair, M. K.; Powell, D. R.; Scadden, M. I. H. C.; Session, C. B.; Tao, J.; Trieu, J.; Whiteford, K. N.; Yuan, Z.; Yun, G.; Zhu, J.; Heemstra, J. M. *J. Org. Chem.* **2016**, *81*, 6816.
- (51) Schoetz, G.; Trapp, O.; Schurig, V. *Anal. Chem.* **2000**, *72*, 2758.
- (52) Schoetz, G.; Trapp, O.; Schurig, V. *Electrophoresis* **2001**, *22*, 2409.
- (53) Trapp, O.; Schoetz, G.; Schurig, V. *Chirality* **2001**, *13*, 403.
- (54) Trapp, O.; Trapp, G.; Schurig, V. *Electrophoresis* **2004**, *25*, 318.
- (55) Trapp, O. *Anal. Chem.* **2006**, *78*, 189.
- (56) Trapp, O. *Electrophoresis* **2007**, *28*, 691.
- (57) Trapp, O. *Electrophoresis* **2010**, *31*, 786.
- (58) Fuessl, S.; Trapp, O. *Electrophoresis* **2012**, *33*, 1060.
- (59) Hruška, V.; Beneš, M.; Svobodová, J.; Zusková, I.; Gaš, B. *Electrophoresis* **2012**, *33*, 938.
- (60) Svobodová, J.; Beneš, M.; Hruška, V.; Ušelová, K.; Gaš, B. *Electrophoresis* **2012**, *33*, 948.
- (61) Hruška, V.; Svobodová, J.; Beneš, M.; Gaš, B. *J. Chrom. A* **2012**, *1267*, 102.
- (62) Benes, M.; Svobodova, J.; Hruska, V.; Dvorak, M.; Zuskova, I.; Gas, B. *J. Chromatogr. A* **2012**, *1267*, 109.
- (63) Xie, S.; Lopez, S. A.; Ramström, O.; Yan, M.; Houk, K. N. *J. Am. Chem. Soc.* **2015**, *137*, 2958.

- 1  
2  
3 (64) Narayanam, M. K.; Liang, Y.; Houk, K. N.; Murphy, J. M. *Chem. Sci.* **2016**, *7*,  
4 1257.  
5 (65) Hohenberg, P.; Kohn, W. *Phys. Rev.* **1964**, *136*, B864.  
6 (66) Kohn, W.; Sham, L. J. *Phys. Rev.* **1965**, *140*, A1133.  
7 (67) Frisch, M. J. T., G. W.; Schlegel, H. B.; Scuseria, G. E.; Robb, M. A.; Cheeseman,  
8 J. R.; Scalmani, G.; Barone, V.; Mennucci, B.; Petersson, G. A.; Nakatsuji, H.; Caricato, M.; Li,  
9 X.; Hratchian, H. P.; Izmaylov, A. F.; Bloino, J.; Zheng, G.; Sonnenberg, J. L.; Hada, M.; Ehara,  
10 M.; Toyota, K.; Fukuda, R.; Hasegawa, J.; Ishida, M.; Nakajima, T.; Honda, Y.; Kitao, O.; Nakai,  
11 H.; Vreven, T.; Montgomery\_Jr., J. A.; Peralta, J. E.; Ogliaro, F.; Bearpark, M.; Heyd, J. J.;  
12 Brothers, E.; Kudin, K. N.; Staroverov, V. N.; Keith, T.; Kobayashi, R.; Normand, J.;  
13 Raghavachari, K.; Rendell, A.; Burant, J. C.; Iyengar, S. S.; Tomasi, J.; Cossi, M.; Rega, N.;  
14 Millam, J. M.; Klene, M.; Knox, J. E.; Cross, J. B.; Bakken, V.; Adamo, C.; Jaramillo, J.;  
15 Gomperts, R.; Stratmann, R. E.; Yazyev, O.; Austin, A. J.; Cammi, R.; Pomelli, C.; Ochterski, J.  
16 W.; Martin, R. L.; Morokuma, K.; Zakrzewski, V. G.; Voth, G. A.; Salvador, P.; Dannenberg, J.  
17 J.; Dapprich, S.; Daniels, A. D.; Farkas, O.; Foresman, J. B.; Ortiz, J. V.; Cioslowski, J.; Fox, D.  
18 J. *Gaussian 09 Revision D.01 ed., Gaussian Inc., Wallingford CT* **2013**.  
19 (68) Stephens, P. J.; Devlin, F. J.; Chabalowski, C. F.; Frisch, M. J. *J. Phys. Chem.*  
20 **1994**, *98*, 11623.  
21 (69) Lee, C.; Yang, W.; Parr, R. G. *Phys. Rev. B* **1988**, *37*, 785.  
22 (70) Becke, A. D. *J. Chem. Phys.* **1993**, *98*, 5648.  
23 (71) Dunning, T. H. *J. Chem. Phys.* **1989**, *90*, 1007.  
24 (72) Woon, D. E.; Dunning, T. H. *J. Chem. Phys.* **1993**, *98*, 1358.  
25 (73) Kendall, R. A.; Dunning, T. H.; Harrison, R. J. *J. Chem. Phys.* **1992**, *96*, 6796.  
26 (74) Grimme, S.; Antony, J.; Ehrlich, S.; Krieg, H. *J. Chem. Phys.* **2010**, *132*, 154104.  
27 (75) Barone, V.; Cossi, M. *J. Phys. Chem. A* **1998**, *102*, 1995.  
28 (76) Cossi, M.; Rega, N.; Scalmani, G.; Barone, V. *J. Comput. Chem.* **2003**, *24*, 669.  
29 (77) Lan, Y.; Zou, L.; Cao, Y.; Houk, K. N. *J. Phys. Chem. A* **2011**, *115*, 13906.  
30 (78) Stefl, M.; Walz, S.; Knop, M.; Trapp, O. *Electrophoresis* **2016**.  
31 (79) Dommerholt, J.; Rutjes, F. P. J. T.; van Delft, F. L. *Top. Curr. Chem.* **2016**, *374*,  
32 16.  
33 (80) Nguyen, D. M.; Miles, D. H. *Synth. Commun.* **2011**, *41*, 1759.  
34 (81) Ryu, B. Y.; Emrick, T. *Macromolecules* **2011**, *44*, 5693.  
35 (82) Hradilova, L.; Polakova, M.; Dvorakova, B.; Hajduch, M.; Petrus, L. *Carbohydr.*  
36 *Res.* **2012**, *361*, 1.  
37 (83) Nonogaki, S.; Toriumi, M. *J. Macromol. Sci. A* **1988**, *25*, 617.  
38  
39  
40  
41  
42  
43  
44  
45  
46  
47  
48  
49  
50  
51  
52  
53  
54  
55  
56  
57  
58  
59  
60

## TOC Graphics

